Bagasse Ash Geopolymer Mortar Containing Limestone Dust And Water Hyacinth Fiber

S. Puttala[1], T. Phantachang[2], P. Chindaprasirt[3], and S. Homwuttiwong[4*]

[1] Department of Civil Engineering and Architecture, Faculty of Industrial Technology, Sakon Nakhon Rajabhat University 47000, Thailand.
[2] Faculty of Engineering, Rajamangala University of Technology Lanna, Chiang Mai 50300, Thailand.
[3] Sustainable Infrastructure Research and Development Center, Department of Civil Engineering, Faculty of Engineering, Khon Kaen University, Khon Kaen, 40002, Thailand, and Academy of Science, Royal Society of Thailand, Dusit, Bangkok, 10300, Thailand.
[4] Faculty of Engineering, Mahasarakham University, Mahasarakham 44150, Thailand.
[*] Corresponding author. E-mail: sahalaph.h@msu.ac.th

Received: Feb. 20, 2025; Accepted: May 14, 2025

This study addresses the critical challenges of construction waste management through the development of an innovative geopolymer mortar using agricultural and industrial waste materials. Using bagasse ash (BA) as the primary precursor and sodium hydroxide with sodium silicate as alkaline activators, the incorporation of water hyacinth fiber (WHF) with 0-5% and limestone dust (LSD) with 20% replacement was systematically investigated. A comprehensive mechanical characterization revealed: (1) the control geopolymer exhibited a compressive strength of 30 MPa after 28 days; (2) the incorporation of 1.25% WHF slightly reduced the compressive strength by 15-20%, while the flexural strength was significantly increased by 80%; (3) high-temperature curing at 100°C accelerated the early strength development to 35 MPa after 7 days, with a slight reduction in strength of 5-8% observed after 28 days. These results highlight the potential of waste-derived materials for the development of sustainable, high-performance composites for construction.

Keywords: Geopolymer; Concrete; Bagasse ash; Limestone dust; Water hyacinth fiber; Waste materials

http://dx.doi.org/10.6180/jase.202603_29(3).0012

1. Introduction

The emission of carbon dioxide is a primary factor in global temperature rise, significantly impacting climate change. The construction industry is one of the major contributors to these emissions, with cement production releasing approximately 0.75 tons of CO_2 for every ton produced [1]. Despite these environmental concerns, urban development continues to drive increasing demand for building materials worldwide. This growing tension between construction needs and environmental sustainability has intensified research into environmentally friendly cementitious alternatives. Industrial and agricultural by-products including fly ash, rice husk ash, silica fume, and blast furnace slag have proven effective as pozzolanic cement substitutes. Furthermore, combining multiple pozzolanic materials often yields enhanced performance properties compared to single-material replacements [2].

The selection of bagasse ash (BA) as a geopolymer precursor is justified by its significant silica content. The, typical ash yields range from 10-25% with silica concentrations between 60-70% [3]. While rice husk ash offers higher ash percentages, BA provides a strategic alternative by utilizing an underexploited agricultural waste stream from Thailand's extensive sugar industry, transforming a low-value by-product into a sustainable construction material. Limestone dust (LSD) primarily consists of calcium carbonate

($CaCO_3$) as its main chemical component [4].

In Thailand, water hyacinth is a major problem in river and canal hindering water flow in water ways. The hyacinth reduces the water flow by up to 40 percent, obstruct boat flow and hinder the growth of aquatic animals. In some cases, flooding is originated due to the presence of water hyacinths. Water hyacinths are fast-growing plants; one water hyacinth plant could grow to 1,000 in a month [5]. Water hyacinth removal requires a lot of efforts including labor expense, and disposal of the weed. Therefore, it is worth finding ways to use water hyacinths to add value and reduce the burden of disposal.

Geopolymer concrete is produced using industrial and agricultural waste materials such as fly ash, slag, rice husk ash and other similar materials. The process involves activating these materials with alkaline solutions such as sodium hydroxide and sodium silicate. However, fly ash and other pozzolanic materials are now valuable since they were introduced to partially replace Portland cement in concrete mixture. Bagasse ash is a waste from the sugar mill industry, and it has a high content of silica [6]. Ground to fine particles, it can also be used to partially replace cement in concrete [7]. However, BA is normally black in color from the presence of high unburnt carbon content. As a result, bagasse ash is still a non-value material and most of it is disposed of in landfills [8]. The study to produce geopolymer from bagasse ash has been reported in recent years. Also, it has been suggested to develop geopolymer from bagasse ash blended with other waste materials [3, 9]. It can be considered a sustainable and environmentally friendly material with many potential applications [10].

Recent studies have demonstrated the potential of geopolymers using waste materials, with Zhang et al. [11] achieved 50 MPa with fly ash and Pradhan, Pradhan et al. [12] reported 38 MPa with rice husk ash, Kumar and Kumar et al. [13] indicating 65% improvement in flexural strength with natural fibers, and Bayiha, B. N. et al. (2019) [14] showing improved density by 8% with limestone fillers. Despite these advances, the combined effect of water hyacinth fibers and limestone dust in bagasse-ash geopolymers is still unexplored.

This research addresses this knowledge gap by developing multi-component geopolymers from bagasse ash (BA) activated with alkaline solutions and enhanced with both water hyacinth fiber and limestone dust. This approach offers dual environmental benefits: utilizing agricultural waste that would otherwise contribute to disposal problems, and substantially reducing CO_2 emissions compared to conventional cement production processes, as demonstrated in similar geopolymer systems [14].

The specific objectives of this study were:

- To analyze the chemical composition and mineralogical properties of bagasse ash and limestone dust for geopolymer synthesis.
- To evaluate the influence of water hyacinth fiber (WHF) content (0%, 1.25%, 2.5%, and 5%) on the mechanical properties of bagasse ash geopolymer mortar.
- To investigate the relationship between WHF content, curing conditions, and resulting compressive and flexural strengths.
- To assess the water absorption characteristics and potential applications of the developed composites.
- To determine the optimal WHF composition for balancing structural performance with environmental benefits.

2. Materials and methods

2.1. Material properties

Raw materials were characterized using XRF for chemical composition analysis, SEM for microstructural examination, specific gravity (ASTM C128), particle size distribution, and loss on ignition (ASTM C114) to establish suitability for geopolymerization.

2.1.1. Bagasse ash (BA)

BA from Saharuang sugar mill in Mukdahan province contains 60.7%SiO_2, 1.3%Al_2O_3, 21.6% Fe_2O_3, 6.1%CaO, and 14.3% LOI. While the main oxides meet Class N pozzolan criteria per ASTM C618-22, the higher LOI results from residual carbon in the raw material [15]. The SEM shows irregular BA particles (Fig. 1a), while LSD contains 22.02%SiO_2, 6.38%Al_2O_3, 2.42% CaO with predominantly spherical particles (Fig. 1b). In alkaline conditions, BA's silica and alumina dissolve to form Si-O-Al networks [16], with calcium ions from both materials forming supplementary C-S-H phases [17]. LSD serves as nucleation sites and micro-fillers [18], though excess amounts hinder geopolymerization [19].

2.1.2. Limestone dust (LSD)

Limestone dust (LSD) improves concrete workability, reduces carbonation and shrinkage [20]. Moderate use is crucial; excessive LSD reduces compressive strength. LSD serves as a filler and density enhancer [21–23]. LSD, a by-product of limestone crushing, was dried, sieved to 850 microns, and analyzed for chemical composition as shown in Table 1. SEM showed mostly rounded LSD particles, as shown in Fig. 1(b).

Table 1. Chemical composition of BA and LSD (by mass).

	Chemical composition (%)								
	SiO_2	Al_2O_3	Fe_2O_3	CaO	K_2O	TiO_2	$\mathbf{MnO_2}$	Other	LOI
BA	60.7	1.3	21.6	6.1	5.2	1.5	1.7	1.9	14.3
LSD	22.02	6.38	2.56	2.42	1.16	0.46	1.13	63.87	10.95

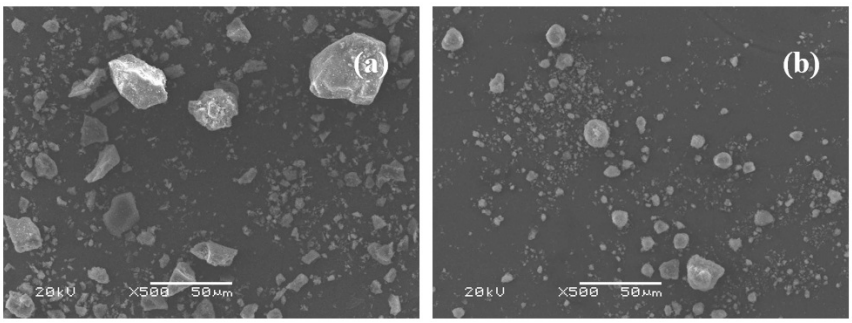

Fig. 1. (a) SEM of bagasse ash (BA), (b) SEM of limestone dust (LSD).

2.1.3. *Water hyacinth fiber (WHF)*

Water hyacinth was collected from the river, cut into $25 - 50$ mm pieces, and subjected to alkaline treatment by immersion in 6M sodium hydroxide solution for 24 hours. This alkaline treatment primarily removed extractives and initiated partial degradation of amorphous components. The treated fibers were subsequently boiled in hot water to remove soluble compounds and residual extractives. The fibers were then cleaned with an alcohol solution and dried in an oven at 100°C. Fourier-transform infrared spectroscopy (FTIR) analysis was performed to verify the partial removal of lignin and hemicellulose, showing characteristic reductions in peaks at 1730 cm^{-1} ($C = O$ stretching in hemicellulose) and 1510 cm^{-1} (aromatic skeletal vibration in lignin) compared to untreated fibers. Residual lignin content was determined to be approximately 12% by weight using the Klason method.

2.1.4. *Alkali solutions*

The alkaline activators were 10 molar sodium hydroxide ($NaOH, NH$) and sodium silicate (Na_2Si_3O, NS). The ratio of the NH solution to the NS solution (NH/NS) was $1 : 1$ and the ratio of alkali solution to solid binder was set at 0.55 . The NH solution was obtained from 98% pure NH pellets. The composition of the NS solution was $29.4\%SiO_2, 14.7\%Na_2O$ and 55.99% water (by mass).

2.1.5. *Aggregates*

Cleaned natural river sand with fineness modulus (FM) of 2.65, specific gravity of 2.62 in a saturated surface dry condition was used as fine aggregate.

2.1.6. *Samples*

Two sizes of test specimens were cast according to the standard [24, 25], a cube of $50 \times 50 \times 50$ mm and a prism of $40 \times 40 \times 160$ mm. The specimens were wrapped in plastic film to prevent moisture from escaping and then cured in an electric oven for 24 hours. Curing samples at $23 \pm 2°C$ for 1 hour, followed by accelerated thermal curing at 40°C and 100°C for 24 hours to enhance geopolymerization [26], then maintained at room temperature until testing age to simulate field conditions.

2.2. Methods

2.2.1. *Mineral composition*

Mechanical properties were tested in accordance with ASTM C109 (compressive strength) and ASTM C348 (flexural strength). Microstructural and chemical analyses included XRD (Cu-Kα, 40 kV, 30 mA) for crystalline phase identification, SEM for interface examination, and FTIR for chemical bonding analysis, particularly to verify WHF incorporation within the geopolymer matrix.

2.2.2. *Mixture of geopolymer mortars*

The mixing methodology is illustrated in the flowchart as shown in Fig. 2. Mixing ratios are detailed in Table 2, where fine aggregate was replaced with 20% LSD, with WHF varying from 0-5% of bagasse ash weight. Sample preparation followed a structured process of dry mixing, wet mixing, and progressive curing to ensure consistent geopolymer mortar formation.

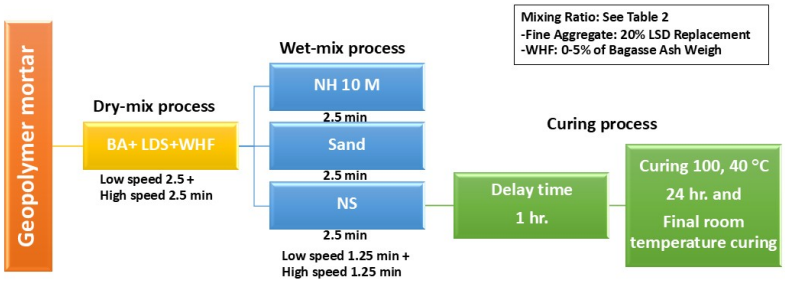

Fig. 2. Flow chart of mixing methodology.

Table 2. Proportions of geopolymer mortar BA blend with WHF.

BA (kg)	NaOH (kg)	Na_2Si_3O (kg)	Sand (kg)	LSD (kg)	WHF (kg)
700	192	192	1,400	0	0 (0%)
700	192	192	1,260	280	8.75 (1.25%)
700	192	192	1,260	280	17.50 (2.50%)
700	192	192	1,260	280	35.00 (5.00%)

3. Results and discussion

3.1. Physical and chemical properties

3.1.1. XRD analysis

The results of XRD analysis of the crystalline structure of compounds and minerals from Fig. 3. The XRD pattern of BA shows sharp peak of SiO_2 (Quartz) at $2\theta = 26°$, indicating the presence of crystalline silica critical for geopolymerization reactions. Similar result was reported by Akbar et al. [27], and small peaks of Al_2O_3 (Alumina) distributed before and after the peak of quartz. For the LSD, the peak value of quartz is 27°2θ. The values for quartz and dolomite are 27° and 29°2θ [28].

3.1.2. The SEM morphologies of WHF

The SEM morphologies of WHF are shown in Fig. 4. The treatment of WHF with alkali leads to the breaking of lignin-ester bonds. Therefore, hemicellulose and cellulose that prevent the breaking of hemicellulose were observed, which is due to the changes in the lignin structure, as shown in Fig. 4(a). The rough surface of the fibers along the entire length [29] is shown in Fig. 4(b), which supports the fiber-matrix adhesion in the geopolymer mortar [30].

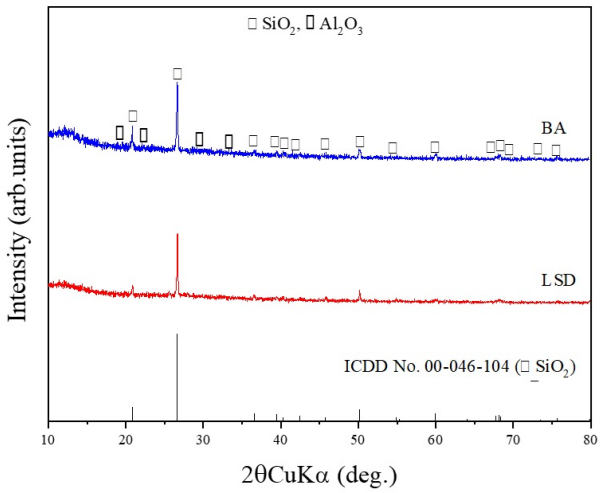

Fig. 3. XRD of bagasse ash and of limestone dust.

3.1.3. FTIR spectra

Fig. 5 shows the FTIR spectra of the absorption bands at 3380 cm^{-1} for WHF corresponding to the hydroxyl group (OH). The absorption band at 2910 cm^{-1} for WHF is attributed to the CH stretching vibration. The absorption band at 1634 and 1638 cm^{-1} in WHF is attributed to the carbonyl group (C = O) of hemicellulose. The alkaline treatment removed hemicellulose, lignin and pectin in the henequen fibers. In addition, the absorption band at 1248 cm^{-1} in WHF disappeared after alkaline treatment. This band is assigned to the C-O stretching of the acetyl group of lignin and was removed by the NaOH treatment [31].

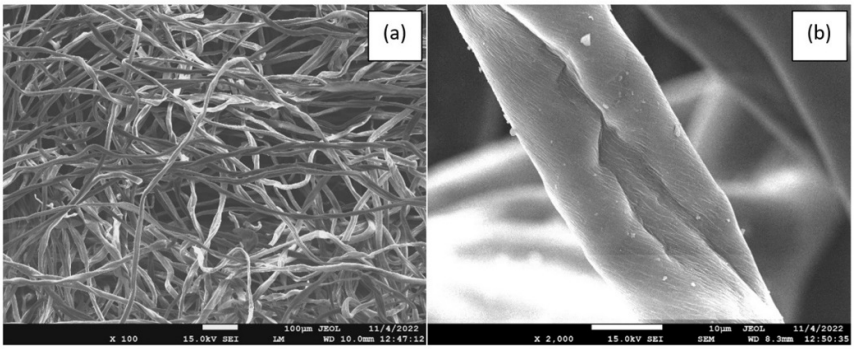

Fig. 4. SEM of hyacinth fiber with magnification of 100x (a) and 2,000x (b).

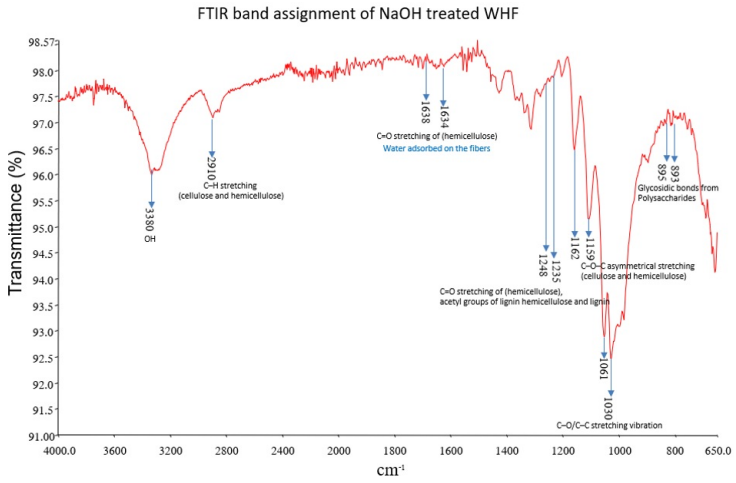

Fig. 5. FTIR spectra for WHF.

3.1.4. X-ray diffraction technique (XRD)

Fig. 6 shows the XRD results with peak intensities ranging from 2800-3700 a.u. (arbitrary- units) for various WHF mixtures. Quartz remains the dominant crystalline phase (ICDD No. 00-046-104), with some minor alumina peaks visible across all samples. The control sample had the highest peak (3700 a.u.), with slight variations in the fiber-reinforced samples, ultimately reaching 3400 a.u. at 5% WHF content. This pattern likely stems from WHF particles creating crystallization sites throughout the matrix, similar to findings by Hemida, Hemida et al. [32]. From the trial test, the use of 5% WHF revealed significant handling problems and fiber clumping, which would have compromised the ability to produce consistent samples.

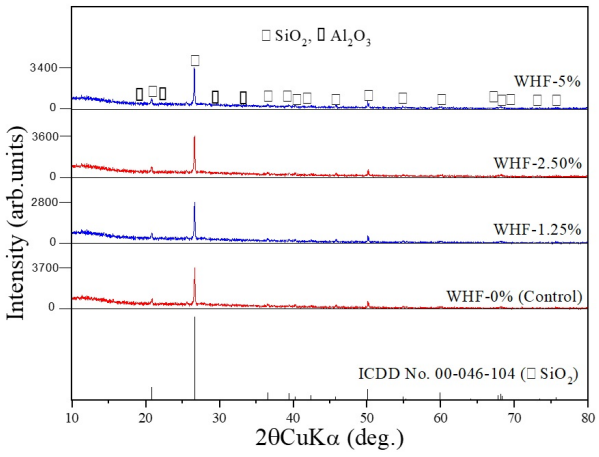

Fig. 6. XRD of geopolymer HWF 0, 1.25%, 2.5% and 5.0%.

3.2. Mechanical properties

3.2.1. Effect of limestone dust (LSD)

Control geopolymers have pores due to limited liquid content. Replacing sand with limestone dust (LSD) decreased pore size and number. The geopolymer containing LSD weighed approximately 13% more than the control, indicating a denser structure. This increased density likely improved properties by reducing pores, enhancing both

mechanical performance and durability.

3.2.2. Water absorption

The water absorption coefficient also increased with the increase in WHF content in the geopolymer mortar, as shown in Fig. 7. This is due to 2 reasons: The fibers create voids and pores inside the geopolymer and the WHF also absorb the water. For the geopolymer sample cured at 40°C, the water absorption coefficient increased uniformly with the increase in fiber content. However, for the sample cured at 100°C, the water absorption coefficient was found to increase significantly when more than 2.5% WHF was used. The results of this experiment suggest that curing at high temperatures damages the interior of the geopolymer.

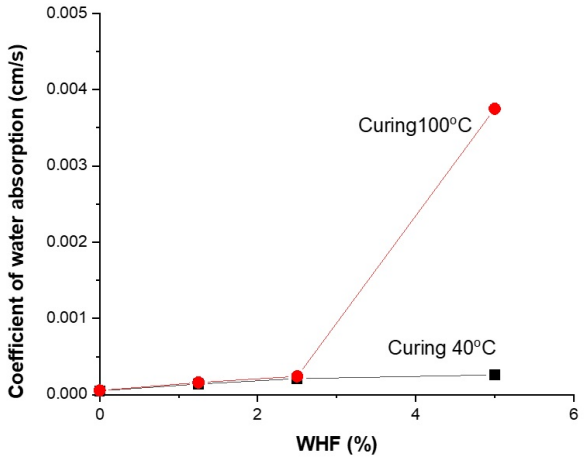

Fig. 7. The coefficient of water absorption and percentage of WHF.

3.2.3. Compressive strength

Fig. 8(a) and (b) show the compressive strength of geopolymer mortar at 7, 14 and 28 days cured at 40°C and 100°C respectively. For the geopolymer without WHF cured at 40°C, the compressive strengths after 7 and 14 days were 9 and 11 MPa , respectively, and increased to 30 MPa after 28 days. The results demonstrate that compressive strength increases with sample age [33] and could continue beyond 28 days, as reported by Sittinun, Sittinun et al. [34] of strength development in moderately cured geopolymers up to 60 days.

However, for 100°C curing, the trend was reversed. The highest compressive strength of 29.5 MPa was reached after 7 days but decreased to 18.5 MPa at 28 days. This strength reduction at later ages with high-temperature curing has been observed in geopolymers made from various pozzolanic materials [35–37]. High-temperature curing can damage the microstructure, causing dehydration and cracking, leading to shrinkage and reduced compressive strength [38–40].

These results clearly indicate that curing temperature directly influences geopolymer strength. According to Detphan, Detphan and Chindaprasirt [41], the optimal curing temperature range for fly ash geopolymers is $60 - 75°C$. The curing temperatures between $40 - 100°C$ might thus be the most suitable curing temperature for bagasse ash-WHF geopolymers.

Statistical analysis of WHF-compressive strength relationship showed significant inverse correlation (ANOVA: $F(3, 16) = 18.42, p < 0.01$). Specimens containing 0%, 1.25%, 2.5%, and 5% WHF exhibited mean compressive strengths at 28 days of 30, 28, 26, and 18 MPa , respectively. Regression analysis revealed a linear model ($R^2 = 0.96$): Compressive strength $= CSo(1 - 0.07WHF\%)$, where CS_o represents initial strength. The volumetric increase caused by WHF incorporation disrupts matrix continuity, aligning with findings by Lv and Liu [42] on fiber-matrix interference mechanisms. Temperature effects were also significant; samples cured at 100°C achieved peak strength (approximately 30 MPa) at 7 days but showed strength reduction at 14 and 28 days, with effect becoming more pronounced over time. This thermal acceleration pattern supports Addis, Addis et al. [43] observations on early geopolymerization kinetics in fiber-reinforced systems.

Adding LSD increased the geopolymer's mass by 13%, creating a tighter internal structure. This density improved strength, chloride resistance, and carbonation protection [44] ideal for marine structures and underground installations. The drawbacks include greater structural weight, higher heat conductivity, and reduced sound absorption [45]. These materials work best in thin, durable structural components but aren't suitable for thermal or acoustic applications, similar to other dense cement systems [46].

Fig. 9(a) compares the tests of samples after 28 days of geopolymers with treated and untreated WHF fibers. It was found that the compressive strength tended to decrease as the percentage of WHF fibers increased for both types. In addition, it was found that increasing the percentage of WHF fibers from 2.5% to 5% resulted in only minor differences in compressive strength when cured at 100°C, as shown in Fig. 9(b).

3.2.4. Flexural strength

The flexural strength of bagasse ash mixed with WHF geopolymers was tested after 28 days. All samples were damaged in the middle by the bending load, which illustrates the effect of the (WHF) fiber inclusions in the geopolymer composites. The flexural strength of the geopolymers without WHF cured at 40°C was 6.5 MPa . The flexu-

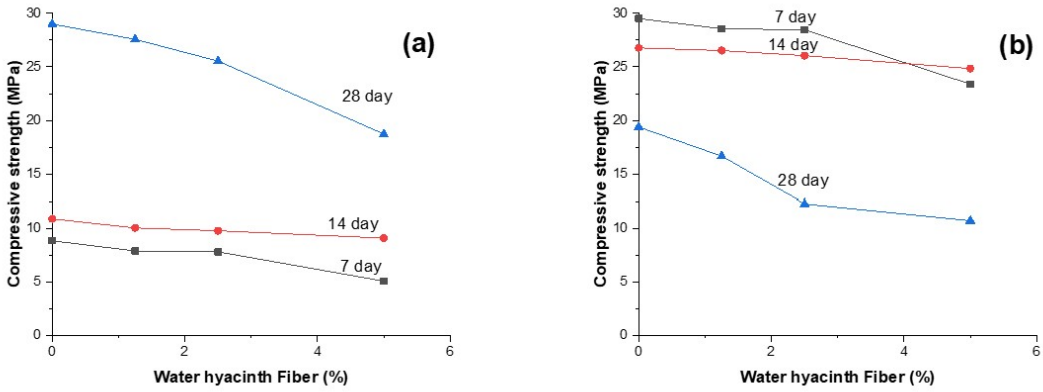

Fig. 8. Compressive strength of curing geopolymer mortar at (a) 40°C and (b) 100°C.

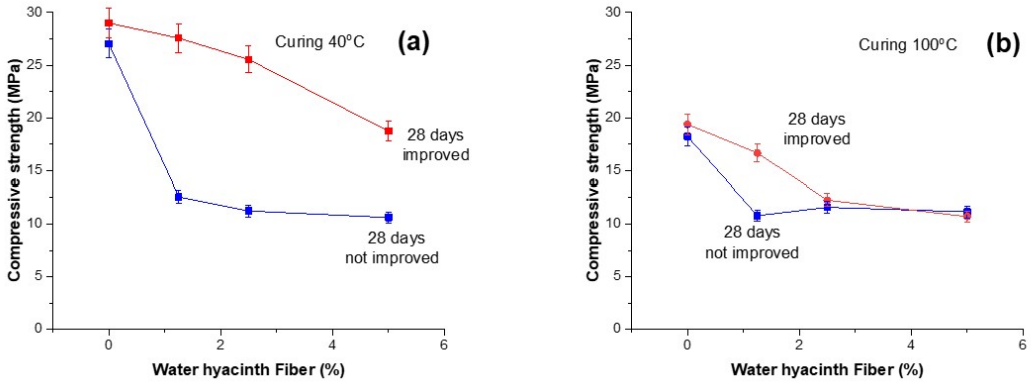

Fig. 9. Compressive strength of geopolymer mortar blend with WHF (a) 40°C and (b) 100°C

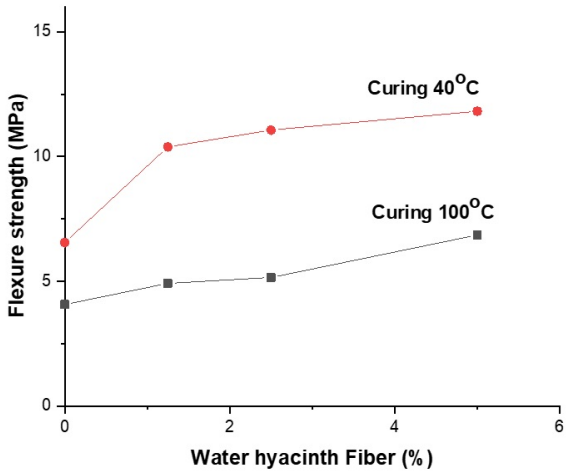

Fig. 10. Flexural strength of geopolymer mortar blend with WHF.

ral strength increased with increasing WHF content and reached a maximum of 11.82 MPa at a WHF content of 5%. This value is higher than 80% compared to the geopolymer without WHF. The results of flexural strength development for the samples cured at 100°C were not as good as those of the samples cured at 40°C. As can be seen in Fig.10, the maximum flexural strength of this group of samples was 6.5 MPa , which is about 40% higher than that of the control samples. This test result clearly shows that the WHF fibers contribute to the improvement of the flexural strength of the geopolymer samples [47]. However, it should be noted that an increase in the fiber content leads to a significant decrease in the compressive strength of the geopolymer. Therefore, the amount of fibers used must be considered appropriately. So that the compressive strength of the geopolymer does not become too low [48].

The flexural performance of geopolymer composites reveals a nuanced relationship between water hyacinth fiber (WHF) concentration and curing temperature. As

WHF content increased from 0% to 5%, a progressive enhancement in flexural strength was observed, attributed to fiber-matrix interactions and temperature-dependent bonding mechanisms. Moderate curing temperatures (40°C) gave superior mechanical properties compared to hightemperature conditions, aligning with recent investigations on sustainable composite materials [13].

Notably, the 5% WHF geopolymer outperformed traditional OPC-natural fiber mortars with nearly 50% higher flexural strength [46]. It also demonstrated a substantial improvement roughly a quarter better than coal fly ash geopolymers [49], while achieving comparable performance to materials reinforced with synthetic fibers [50]. For the key advantage. The composite relies entirely on agricultural waste. Tests revealed exceptional crack-bridging behavior, with strain-at-break exceeding conventional fiber-reinforced mortars by approximately 35% [13]. While statistical analysis confirmed WHF's significant flexural benefits, an expected trade-off in compressive strength following CS_0 (1-0.08 WHF%) was observed. Interestingly, this trade-off pattern aligns with Khan et al. [51] findings, though the obtained formulation achieved superior flexural gains.

4. Conclusions

From the experimental study conducted, the following conclusions could be made.

1. The X-ray diffraction (XRD) technique of the substrate shows the peak of quartz with the chemical composition of silicon and oxygen and aluminum oxide with the chemical composition of aluminum oxide (Al_2O_3). The peak limestone dust of the mineral calcite has the chemical composition of calcium carbonate $(CaCO_3)$ with alkaline properties suitable for use in geopolymers.

2. The addition of WHF resulted in a reduction the compressive strength of geopolymer. Among the tested ratios ($0\%, 1.25\%, 2.5\%$, and 5%), the optimum ratio of 1.25% WHF in geopolymer mortar provides the best compressive strength at 28 days for curing at low temperatures. This offers benefits in crack reduction and waste utilization with approximately $3-5\%$ material cost savings, making it promising for large-scale industrial applications.

3. The use of fibers led to a significant increase in flexural strength. This was particularly true for samples that were cured at low temperatures. The flexural strength of the geopolymer increases with increasing WHF content and could be up to 80% compared to the control geopolymer.

4. The water absorption coefficient of geopolymer mortar tends to increase with the increase in the proportion of WHF due to the high absorption character of the fiber.

5. The obtained results reveal optimal applications based on WHF content: specimens with 1.25% WHF maintain acceptable structural properties while enhancing flexural performance suitable for prefabricated panels and specialized pavements [52]; whereas higher fiber contents (2.5% and 5%) excel in non-load-bearing applications [13]. The testing at these specific WHF percentages (0%, 1.25%, 2.5%, and 5%) demonstrated a clear inverse relationship between fiber content and compressive strength, establishing practical structural limitations. Future development could explore hybrid reinforcement strategies incorporating banana fiber [53] or matrix modifications to better balance mechanical performance with environmental benefits.

Acknowledgements

This research was supported by the TRF Research Career Development Grant, Sakon Nakhon Rajabhat University, 2026. The authors would also like to thank the Materials Testing Centre of the Department of Civil Engineering and Architecture, Faculty of Industrial Engineering: Sakon Nakhon Rajabhat University.

References

[1] B. Liu, J. Qin, J. Shi, J. Jiang, X. Wu, and Z. He, (2021) *"New perspectives on utilization of CO2 sequestration technologies in cement-based materials"* **Construction and Building Materials *272***: 121660. DOI: 10.1016/j.conbuildmat.2020.121660.

[2] A. Ahmed, (2024) *"Assessing the effects of supplementary cementitious materials on concrete properties: a review"* **Discover Civil Engineering *1***(1): 1–47. DOI: 10.1007/s44290-024-00154-z.

[3] M. Amran, S. Debbarma, and T. Ozbakkaloglu, (2021) *"Fly ash-based eco-friendly geopolymer concrete: A critical review of the long-term durability properties"* **Construction and Building Materials *270***: 121857. DOI: 10.1016/j.conbuildmat.2020.121857.

[4] Y.-Y. Tsai, C. I. Vazquez, R.-F. Shiu, A. K. Garcia, C. Le, P. Patel, M. Sadqi, and W.-C. Chin, (2021) *"Effects of Rock Dust Particles on Airway Mucus Viscosity"* **Biotechnology and Bioprocess Engineering *26***: 427–434. DOI: 10.1007/s12257-020-0236-x.

[5] L. K. Wang, M.-H. S. Wang, and N. K. Shammas. "Agricultural waste treatment by water hyacinth aquaculture, wetland aquaculture, evapotranspiration, rapid rate land treatment, slow rate land treatment, and subsurface infiltration". In: *Waste Treatment in the Biotechnology, Agricultural and Food Industries: Volume 1*. Springer, 2022, 277–316. DOI: 10.1007/978-3-031-03591-3_6.

[6] L. A. September, N. Kheswa, N. S. Seroka, and L. Khotseng, (2023) *"Green synthesis of silica and silicon from agricultural residue sugarcane bagasse ash–a mini review"* **RSC advances *13***(2): 1370–1380. DOI: 10.1039/d2ra07490g.

[7] S. E. L. Gudia, A. W. Go, M. B. Giduquio, R. G. Juanir, J. B. Jamora, C. Gunarto, and I. D. F. Tabañag, (2023) *"Sugarcane bagasse ash as a partial replacement for cement in paste and mortar formulation–A case in the Philippines"* **Journal of Building Engineering *76***: 107221. DOI: 10.1016/j.jobe.2023.107221.

[8] K. Vimal, K. Churi, and J. Kandasamy, (2022) *"Analysing the drivers for adoption of industry 4.0 technologies in a functional paper–cement–sugar circular sharing network"* **Sustainable Production and Consumption *31***: 459–477. DOI: 10.1016/j.spc.2022.03.006.

[9] N. Chuewangkam, T. Nachaithong, N. Chanlek, P. Thongbai, and S. Pinitsoontorn, (2022) *"Mechanical and dielectric properties of fly ash geopolymer/sugarcane bagasse ash composites"* **Polymers *14***(6): 1140. DOI: 10.3390/polym14061140.

[10] N. N. Khalid, W. K. Al-Saraj, H. F. Naji, et al., (2021) *"Behavior of MK-based Geopolymer Concrete Circular Columns Exposed to Fire"* **Journal of Applied Science and Engineering *24***(1): 91–97. DOI: 10.6180/jase.202102_24(1).0012.

[11] H. Zhang, Q. Zhang, M. Zhang, S. Tang, Y. Pei, F. Skoczylas, and S. Feng, (2024) *"Effect of fly ash and metakaolin on the mechanical properties and microstructure of magnesium ammonium phosphate cement paste"* **Construction and Building Materials *424***: 135871. DOI: 10.1016/j.conbuildmat.2024.135871.

[12] S. S. Pradhan, S. Pramanik, U. Mishra, S. K. Biswal, and S. Thapa, (2023) *"Effect of RHA on mechanical properties of GGBS based alkali activated concrete: an experimental and statistical modelling"* **Russian Journal of Nondestructive Testing *59***(7): 767–784. DOI: 10.1134/S1061830923600375.

[13] S. Kumar, L. Prasad, V. K. Patel, V. Kumar, A. Kumar, and A. Yadav, (2022) *"Physico-mechanical properties and Taguchi optimized abrasive wear of alkali treated and fly ash reinforced Himalayan agave fiber polyester composite"* **Journal of Natural Fibers *19***(14): 9269–9282. DOI: 10.1080/15440478.2021.1982818.

[14] B. S. Thomas, J. Yang, K. H. Mo, J. A. Abdalla, R. A. Hawileh, and E. Ariyachandra, (2021) *"Biomass ashes from agricultural wastes as supplementary cementitious materials or aggregate replacement in cement/geopolymer concrete: A comprehensive review"* **Journal of Building Engineering *40***: 102332. DOI: 10.1016/j.jobe.2021.102332.

[15] A. International. *ASTM C618-22, Standard Specification for Coal Fly Ash and Raw or Calcined Natural Pozzolan for Use in Concrete*. 2022.

[16] P. Chindaprasirt and U. Rattanasak, (2020) *"Eco-production of silica from sugarcane bagasse ash for use as a photochromic pigment filler"* **Scientific reports *10***(1): 9890. DOI: 10.1038/s41598-020-66885-y.

[17] I. Phummiphan, S. Horpibulsuk, R. Rachan, A. Arulrajah, S.-L. Shen, and P. Chindaprasirt, (2018) *"High calcium fly ash geopolymer stabilized lateritic soil and granulated blast furnace slag blends as a pavement base material"* **Journal of hazardous materials *341***: 257–267. DOI: 10.1016/j.jhazmat.2017.07.067.

[18] Y.-C. Choi, (2024) *"Degree of Hydration, Microstructure, and Mechanical Properties of Cement-Modified TiO2 Nanoparticles"* **Materials *17***(18): 4541. DOI: 10.3390/ma17184541.

[19] B. N. Bayiha, N. Billong, E. Yamb, R. C. Kaze, and R. Nzengwa, (2019) *"Effect of limestone dosages on some properties of geopolymer from thermally activated halloysite"* **Construction and Building Materials *217***: 28–35. DOI: 10.1016/j.conbuildmat.2019.05.058.

[20] Z. Jiang, Q. Yang, B. Wang, C. Li, J. Zhang, and Q. Ren, (2024) *"Limestone filler as a mineral additive on the compressive strength and durability of self-compacting concrete with limestone manufactured sand"* **Journal of Building Engineering *94***: 109965. DOI: 10.1016/j.jobe.2024.109965.

[21] G. Fares, M. H. Albaroud, and M. I. Khan, (2020) *"Fine limestone dust from ornamental stone factories: a potential filler in the production of High-Performance Hybrid Fiber-Reinforced Concrete"* **Construction and Building Materials *262***: 120009. DOI: 10.1016/j.conbuildmat.2020.120009.

[22] R. Alyousef, W. Abbass, F. Aslam, and S. A. A. Gillani, (2023) *"Characterization of high-performance concrete using limestone powder and supplementary fillers in binary and ternary blends under different curing regimes"* **Case Studies in Construction Materials *18***: e02058. DOI: 10.1016/j.jobe.2023.106180.

[23] R. Alyousef, W. Abbass, F. Aslam, and S. A. A. Gillani, (2023) *"Characterization of high-performance concrete using limestone powder and supplementary fillers in binary and ternary blends under different curing regimes"* **Case Studies in Construction Materials *18***: e02058. DOI: 10.1016/j.cscm.2023.e02058.

[24] A. ASTM. *C109/C109M-16a Standard Test Method for Compressive Strength of Hydraulic Cement Mortars (Using 2-in. or [50-mm] Cube Specimens), ASTM International, West Conshohocken, PA, 2016*. 2017.

[25] ASTM. *ASTM C348-14*. 2014.

[26] B.-h. Mo, H. Zhu, X.-m. Cui, Y. He, and S.-y. Gong, (2014) *"Effect of curing temperature on geopolymerization of metakaolin-based geopolymers"* **Applied clay science *99***: 144–148. DOI: 10.1016/j.clay.2014.06.024.

[27] A. Akbar, F. Farooq, M. Shafique, F. Aslam, R. Alyousef, and H. Alabduljabbar, (2021) *"Sugarcane bagasse ash-based engineered geopolymer mortar incorporating propylene fibers"* **Journal of Building Engineering *33***: 101492. DOI: 10.1016/j.jobe.2020.101492.

[28] J. L. Pastor, R. Tomás, M. Cano, A. Riquelme, and E. Gutiérrez, (2019) *"Evaluation of the improvement effect of limestone powder waste in the stabilization of swelling clayey soil"* **Sustainability *11***(3): 679. DOI: 10.3390/su11030679.

[29] H. Abral, D. Kadriadi, A. Rodianus, P. Mastariyanto, S. Arief, S. Sapuan, M. R. Ishak, et al., (2014) *"Mechanical properties of water hyacinth fibers–polyester composites before and after immersion in water"* **Materials & Design *58***: 125–129. DOI: 10.1016/j.matdes.2014.01.043.

[30] S. Tan and A. Supri, (2016) *"Properties of low-density polyethylene/natural rubber/water hyacinth fiber composites: the effect of alkaline treatment"* **Polymer Bulletin *73***: 539–557. DOI: 10.1007/s00289-015-1508-z.

[31] N. H. Sari, E. Syafri, W. Fatriasari, A. Karimah, et al., (2024) *"Biocomposites Based On Micro Cellulose Fibers Extracted From Paederia Foetida Stems And Investigation Of Important Properties"* **Journal of Applied Science and Engineering *27***(9): 3261–3272. DOI: 10.6180/jase.202409_27(9).0015.

[32] M. H. Hemida, H. Moustafa, S. Mehanny, M. Morsy, A. Dufresne, E. N. A. E. Rahman, and M. Ibrahim, (2023) *"Cellulose nanocrystals from agricultural residues (Eichhornia crassipes): Extraction and characterization"* **Heliyon *9***(6): DOI: 10.1016/j.heliyon.2023.e16436.

[33] S. Puttala, W. Hiranphattararoj, and S. Homwuttiwong, (2021) *"Development of a geopolymer made from bagasse ash for use a cementitious material"* **Asia-Pacific Journal of Science and Technology *26***(4): 10. DOI: 10.14456/apst.2021.31.

[34] A. Sittinun, P. Pisitsak, and S. Ummartyotin, (2020) *"Improving the oil sorption capability of porous polyurethane composites by the incorporation of cellulose fibers extracted from water hyacinth"* **Composites Communications *20***: 100351. DOI: 10.1016/j.coco.2020.04.017.

[35] S. Puttala, M. Ongwandee, K. Homwutthiwong, and S. Homwuttiwong, (2022) *"STRENGTH ENHANCEMENT BY COMBINED THE CALCINED WATER SUPPLY SLUDGE IN BAGASSE ASH GEOPOLYMER CONCRETE"*:

[36] K.-H. Yang, A.-R. Cho, and J.-K. Song, (2012) *"Effect of water–binder ratio on the mechanical properties of calcium hydroxide-based alkali-activated slag concrete"* **Construction and Building Materials *29***: 504–511. DOI: 10.1016/j.conbuildmat.2011.10.062.

[37] P. Sukmak, S. Horpibulsuk, S.-L. Shen, P. Chindaprasirt, and C. Suksiripattanapong, (2013) *"Factors influencing strength development in clay–fly ash geopolymer"* **Construction and Building Materials *47***: 1125–1136. DOI: 10.1016/j.conbuildmat.2013.05.104.

[38] J. Wongpa, K. Kiattikomol, C. Jaturapitakkul, and P. Chindaprasirt, (2010) *"Compressive strength, modulus of elasticity, and water permeability of inorganic polymer concrete"* **Materials & Design *31***(10): 4748–4754. DOI: 10.1016/j.matdes.2010.05.012.

[39] P. Sajan, T. Jiang, C. Lau, G. Tan, and K. Ng, (2021) *"Combined effect of curing temperature, curing period and alkaline concentration on the mechanical properties of fly ash-based geopolymer"* **Cleaner Materials *1***: 100002. DOI: 10.1016/j.clema.2021.100002.

[40] M. Muracchioli, G. Menardi, M. D'Agostini, G. Franchin, and P. Colombo, (2023) *"Modeling the compressive strength of metakaolin-based geopolymers based on the statistical analysis of experimental data"* **Applied Clay Science *242***: 107020. DOI: 10.1016/j.clay.2023.107020.

[41] S. Detphan and P. Chindaprasirt, (2009) *"Preparation of fly ash and rice husk ash geopolymer"* **International Journal of Minerals, Metallurgy and Materials *16***(6): 720–726. DOI: 10.1016/S1674-4799(10)60019-2.

[42] C. Lv and J. Liu, (2023) *"Alkaline degradation of plant fiber reinforcements in geopolymer: a review"* **Molecules *28***(4): 1868. DOI: 10.3390/molecules28041868.

[43] L. B. Addis, Z. B. Sendekie, and N. Satheesh, (2022) *"Degradation Kinetics and Durability Enhancement Strategies of Cellulosic Fiber-Reinforced Geopolymers and Cement Composites"* **Advances in Materials Science and Engineering *2022***(1): 1981755. DOI: 10.1155/2022/1981755.

[44] H. Qu, M. Feng, M. Li, D. Tian, Y. Zhang, X. Chen, and G. Li, (2023) *"Enhancing the carbonation and chloride resistance of concrete by nano-modified eco-friendly water-based organic coatings"* **Materials Today Communications *37***: 107284. DOI: 10.1016/j.mtcomm.2023.107284.

[45] T. S. Tie, K. H. Mo, A. Putra, S. C. Loo, U. J. Alengaram, and T.-C. Ling, (2020) *"Sound absorption performance of modified concrete: A review"* **Journal of Building Engineering *30***: 101219. DOI: 10.1016/j.jobe.2020.101219.

[46] S. Sharma, P. Sudhakara, J. Singh, S. Singh, and G. Singh, (2023) *"Emerging progressive developments in the fibrous composites for acoustic applications"* **Journal of Manufacturing Processes *102***: 443–477. DOI: 10.1016/j.jmapro.2023.07.053.

[47] S. Niyasom and N. Tangboriboon, (2021) *"Development of biomaterial fillers using eggshells, water hyacinth fibers, and banana fibers for green concrete construction"* **Construction and Building Materials *283***: 122627. DOI: 10.1016/j.conbuildmat.2021.122627.

[48] A. Wongsa, R. Kunthawatwong, S. Naenudon, V. Sata, and P. Chindaprasirt, (2020) *"Natural fiber reinforced high calcium fly ash geopolymer mortar"* **Construction and Building Materials *241***: 118143. DOI: 10.1016/j.conbuildmat.2020.118143.

[49] X. Han, P. Zhang, Y. Zheng, and J. Wang, (2023) *"Utilization of municipal solid waste incineration fly ash with coal fly ash/metakaolin for geopolymer composites preparation"* **Construction and Building Materials *403***: 133060. DOI: 10.1016/j.conbuildmat.2023.133060.

[50] D. K. Rajak, P. H. Wagh, and E. Linul, (2022) *"A review on synthetic fibers for polymer matrix composites: performance, failure modes and applications"* **Materials *15***(14): 4790. DOI: 10.3390/ma15144790.

[51] M. A. Khan, B. Zhang, M. Ahmad, M. Niekurzak, M. S. Khan, M. M. Sabri Sabri, and W. Chen, (2025) *"Optimizing concrete sustainability with bagasse ash and stone dust and its impact on mechanical properties and durability"* **Scientific reports *15***(1): 1385. DOI: 10.1038/s41598-025-85363-x.

[52] D. Glavas, G. Grolleau, and N. Mzoughi, (2023) *"Greening the greenwashers–How to push greenwashers towards more sustainable trajectories"* **Journal of Cleaner Production *382***: 135301. DOI: 10.1016/j.jclepro.2022.135301.

[53] P. Sangkeaw, N. Phoeychawee, C. Thongchom, J. Lawaongkerd, S. Keawsawasvong, and C. Suksiripattanapong, (2024) *"Alkaline Pretreatment Of Banana Pseudostem Waste For Green Cellulose Fiber Composite Materials"* **Journal of Applied Science and Engineering *28***(2): 399–409. DOI: 10.6180/jase.202502_28(2).0018.